C. Alex Goddard, Eric I. Knudsen and John R. Huguenard

You might find this additional information useful...

This article cites 46 articles, 24 of which you can access free at:
http://jn.physiology.org/cgi/content/full/98/6/3486#BIBL

Updated information and services including high-resolution figures, can be found at:
http://jn.physiology.org/cgi/content/full/98/6/3486

Additional material and information about *Journal of Neurophysiology* can be found at:
http://www.the-aps.org/publications/jn

This information is current as of January 25, 2008 .

Intrinsic Excitability of Cholinergic Neurons in the Rat Parabigeminal Nucleus

C. Alex Goddard,[1] Eric I. Knudsen,[1] and John R. Huguenard[2]

[1]*Departments of Neurobiology and* [2]*Neurology, Stanford University, Stanford, California*

Goddard CA, Knudsen EI, Huguenard JR. Intrinsic excitability of cholinergic neurons in the rat parabigeminal nucleus. *J Neurophysiol* 98: 3486–3493, 2007. First published September 26, 2007; doi:10.1152/jn.00960.2007. Cholinergic neurons in the parabigeminal nucleus of the rat midbrain were studied in an acute slice preparation. Spontaneous, regular action potentials were observed both with cell-attached patch recordings as well as with whole cell current-clamp recordings. The spontaneous activity of parabigeminal nucleus (PBN) neurons was not due to synaptic input as it persisted in the presence of the pan-ionotropic excitatory neurotransmitter receptor blocker, kynurenic acid, and the cholinergic blockers dihydro-beta-erythroidine (DHβE) and atropine. This result suggests the existence of intrinsic currents that enable spontaneous activity. In voltage-clamp recordings, I_H and I_A currents were observed in most PBN neurons. I_A had voltage-dependent features that would permit it to contribute to spontaneous firing. In contrast, I_H was significantly activated at membrane potentials lower than the trough of the spike afterhyperpolarization, suggesting that I_H does not contribute to spontaneous firing of PBN neurons. Consistent with this interpretation, application of 25 μM ZD-7288, which blocked I_H, did not affect the rate of spontaneous firing in PBN neurons. Counterparts to I_A and I_H were observed in current-clamp recordings: I_A was reflected as a slow voltage ramp observed between action potentials and on release from hyperpolarization, and I_H was reflected as a depolarizing sag often accompanied by rebound spikes in response to hyperpolarizing current injections. In response to depolarizing current injections, PBN neurons fired at high frequencies, with relatively little accommodation. Ultimately, the spontaneous activity in PBN neurons could be used to modulate cholinergic drive in the superior colliculus in either positive or negative directions.

INTRODUCTION

The parabigeminal nucleus (PBN, also known as Ch8) is a cholinergic midbrain nucleus that is strongly interconnected with the superior colliculus (SC). The SC is a mammalian multisensory structure (Drager and Hubel 1975) that is involved in gaze control and spatial attention (Isa 2002; Muller et al. 2005). Exogenously applied acetylcholine (ACh), a neurotransmitter thought to be crucial for attention (Hasselmo and McGaughy 2004), alters synaptic transmission in the SC of rodents (Endo et al. 2005; Lee et al. 2001; Li et al. 2004) and also reduces saccade latency in monkeys (Aizawa et al. 1999). The majority of cholinergic input to the SC originates in the PBN (Mufson et al. 1986; Sherk 1979; Tokunaga and Otani 1978). An analogous cholinergic nucleus, the nucleus isthmi pars parvocellularis, is present in nonmammalian vertebrates and innervates the nonmammalian counterpart to the SC, the optic tectum (Maczko et al. 2006; Wang et al. 2006).

The connections between the SC and PBN are reciprocal and topographic (Graybiel 1978; Mufson et al. 1986; Sherk 1979; Tokunaga and Otani 1978). The two areas are so densely interconnected that the PBN has been referred to as a satellite of the SC. In addition, the PBN also projects to other brain structures such as the thalamus (Harting et al. 1986; Hashikawa et al. 1986) and the amygdala (Usunoff et al. 2006). Although it has been proposed that this nucleus may help orchestrate long-range excitation or inhibition spanning across the SC (Lee and Hall 2006), it is unknown how the PBN functions to modulate neurons in the SC or in other target regions.

The properties of PBN neurons have been studied in vivo. These neurons fire at a high-frequency in response to visual input (Sherk 1979) but also show high rates of spontaneous activity (Cui and Malpeli 2003; Sherk 1979). This spontaneous activity could allow the PBN to modulate SC activity both up and down. It is unknown if this spontaneous activity is due to extrinsic inputs, intrinsic connections between PBN neurons or to the biophysical properties of PBN neurons themselves. To address these possibilities, we performed cell-attached and whole cell patch-clamp recordings from PBN neurons in an acute, brain slice preparation of the rat midbrain. Here we present the first basic characterization of synaptic and intrinsic currents in PBN neurons. We report that PBN neurons in the slice fire spontaneous action potentials, even in the presence of synaptic blockers and that voltage-activated currents may play a role in regulating this spontaneous activity.

METHODS

Recordings

All animals were treated in accordance to institutional guidelines. Twenty-four Sprague-Dawley rats, aged p18–p23, were anesthetized with pentobarbital (50 mg/kg) and decapitated, and the brains were removed and immersed in a "cutting" solution (4°C) containing (in mM) 234 sucrose, 11 glucose, 24 $NaHCO_3$, 2.5 KCl, 1.25 NaH_2PO_4, 10 $MgSO_4$, and 0.5 $CaCl_2$, aerated with 95% O_2-5% CO_2. Transverse slices (350 μm) were cut with a vibrating slicer (Leica VT1000S). Slices were incubated in oxygenated artificial cerebrospinal fluid (ACSF) containing (in mM) 126 NaCl, 26 $NaHCO_3$, 2.5 KCl, 1.25 NaH_2PO_4, 2 $MgSO_4$, 2 $CaCl_2$, and 10 glucose (pH 7.4), initially at 32°C for 30 min and subsequently at room temperature for a minimum of 30 min before being transferred to the recording chamber. Most recordings were obtained at room temperature. In some cases, the temperature of ACSF flowing in the recording chamber was increased to 32°C by preheating the ACSF via a heat exchanger and recirculating water bath (NES Lab, GP-100).

PBN neurons were visually identified using oblique illumination and video microscopy. Neuronal density and large somatic size were used to distinguish the PBN from surrounding areas. In initial experiments, intracellular labeling with biocytin was used to confirm the morphology and location of recorded neurons. Immunostaining for choline acetyltransferase (ChAT) was used to verify the location of the PBN.

Borosilicate glass electrodes (OD: 1.5 mm, ID: 0.84 mm) were pulled with a Sutter p97 electrode puller to a tip resistance of 2–6 $M\Omega$. For most cell-attached and all whole cell recordings, electrodes were filled with an intracellular solution containing (in mM) 130 K gluconate, 10 KCl, 2 NaCl, 10 HEPES, and 10 EGTA; pH = 7.3 corrected with KOH; 265–280 mosM. Biocytin (0.2%, Sigma, B4261) was included in the intracellular solution for most recordings. Electrodes were filled with ACSF for some cell-attached recordings. In whole cell recordings, the average input resistance was 116 ± 86 $M\Omega$. Resting potential was not able to quantified as neurons were continually spiking.

Drugs were delivered by bath application at the following concentrations: kynurenic acid (1–2 mM, Sigma, k3375); dihydro-beta-erythroidine (DHβE, 100 nM, Sigma, D149); atropine (1 μM, Sigma, A0257); 6,7-dinitroquinoxaline-2,3-dione (DNQX, 12–25 μM, Tocris, 2312); gabazine (5–10 μM, Sigma, s106); 4-aminopyridine (4-AP, 1 and 2 mM, Sigma, A0152); and ZD-7288 (25 μM, Tocris, 1000). Signals were amplified using a Multiclamp 700A patch-clamp amplifier (Axon Instruments), filtered at 3 kHz, sampled at 10 kHz, and acquired using pClamp 9.2 (Axon Instruments). Data analysis was performed using pClamp and Matlab (Mathworks) software.

Data analysis and statistics

Values shown in text and figures are mean $\pm$ SD (not SE). Spike rates and intrinsic currents were detected and analyzed using Clampfit 9.2 software (Molecular Devices). I_H was quantified in voltage-clamp recordings by calculating the difference between the average current over a 50-ms period at two time points: 50 ms after the initiation of a hyperpolarizing step and at the end of the 1-s hyperpolarizing step. To assess blockade of I_H with ZD-7288, sag in potential observed in current-clamp recordings was quantified by calculating the difference between the average membrane voltage over a 100-ms period at two time points: 200 ms after the initiation of hyperpolarizing current injection and at the end of the 1-s hyperpolarizing current injection. To assess the effect of ZD-7288, traces that exhibited a similar initial hyperpolarization after a hyperpolarizing current injection in control and drug conditions were compared. The initial hyperpolarizations of control and ZD-7288 conditions were not significantly different (control: -97.0 ± 6.7 mV and ZD-7288: -99.3 ± 7.2 mV, $P = 0.14$, paired, 2-tailed t-test). I_H deinactivation was fit to the following equation: $I = 2.38 - 0.007 * 0.93^{Vm}$ ($r^2 = 0.99$).

The initial activation range for I_A was determined by applying 100-ms membrane potential conditioning pulses to -110 mV for 100 ms to remove inactivation followed by test voltage steps to progressively more depolarized potentials until I_A was observed. The steady-state I_A inactivation curve was performed at the most depolarized test potential that did not cause elicit escaped action currents. The peak I_A was measured starting 15 ms after returning to the activation voltage for a period of 15 ms; this time period captured the peak of the I_A response. Peak I_A occurred at 25 ± 3 ms after returning to the activation voltage in a sample of seven neurons. For the 4-AP experiments, a lower activation potential was required for assessing I_A; after application of 1 mM 4-AP, depolarization to the most depolarized I_A activation potential in control often led to spikes being generated in voltage clamp. The inactivation curve for each cell was then fit to a Boltzmann function (Origin 7, Northampton, MA).

Histology and immunostaining

Slices containing biocytin–filled neurons were immersed in 4% paraformaldehyde in phosphate-buffered saline (PBS) and kept at 4°C overnight. The following day, the paraformaldehyde was replaced with PBS, and unsectioned slices were incubated at 4°C until tissue processing. To visualize biocytin-filled neurons, slices were washed twice with PBS +0.2% Tween-20 (PBST). Avidin D conjugated to Fluorescein (Vector Labs) was added at 1/100 to the slices for 1.5 h. Sections were then washed twice in PBST, followed by a 30-min incubation with Nissl Red (Molecular Probes) at 1/100, and three more washes of PBST. Slices were washed once in PBS with no Tween, and then mounted onto slides and coverslipped using Vectashield Mounting Medium (Vector Labs).

For ChAT staining, paraformaldehyde fixed slices were washed in PBS and then placed in a solution of 30% sucrose in PBS for 1 h. Slices were resectioned at 50 μm with a freezing microtome and the sections were placed into PBS. The sections were then placed in a blocking solution of 5% goat serum in PBS for 1 h. Mouse anti-rat ChAT antibody (Chemicon, MAB305) was added at 1/100 in blocking solution for 1 day at room temperature and 2 more days at 4°C. Sections were then washed four times with PBS, and goat anti-mouse Alexa Fluor 488 (Molecular Probes, A11001) was added at 1/400 in blocking solution for 1.5 h. Sections were then washed twice in PBS, followed by a 30-min incubation with Nissl Red (Molecular Probes) at 1/100, and three more washes in PBS. Sections were mounted onto slides and coverslipped using Vectashield Mounting Medium.

Microscopy

Slices were imaged at lower power (up to ×20) with a Nikon E800 upright microscope and Zeiss Axiocam and at high power (at least ×40) with a Leica TCS SP2 confocal system.

RESULTS

Morphological studies

The PBN appears as a bump along the lateral wall of the midbrain, just ventral to the brachium of the inferior colliculus (Fig. 1A). It is a cell-dense region devoid of dense fiber tracts. The morphologies of biocytin-filled neurons from this region (Fig. 1B) were similar to previous descriptions of PBN neurons in Golgi studies (Tokunaga and Otani 1978). The dendrites of most neurons were oriented toward the lateral wall of the midbrain (Fig. 1B, left neuron), although some had dendrites oriented along the dorsoventral dimension (Fig. 1B, right neuron). The latter are consistent with the "cylindrical shape" according to the classification of Tokunaga and Otani (1978).

Nearly all of the large, neuronal-like somata of cells in the PBN were ChAT positive (Fig. 1C, left), consistent with previous reports (Mufson et al. 1986). The neuropil also exhibited some ChAT-positive immunoreactivity. On the other hand, very few cells in the neighboring perilemniscal nucleus (PL) exhibited α ChAT immunoreactivity (Fig. 1C, right). Thus our anatomical findings are in agreement with previous reports.

PBN neurons fire spontaneously in vitro

In cell-attached patch recordings, PBN neurons in vitro fired spontaneous, regular action potentials (50/60 neurons, Fig. 2). The average firing rate in cell-attached recording was 2.81 ± 2.15 Hz ($n = 50$). Spontaneous firing persisted in most experiments (15 of 17 neurons) where cell-attached recordings were
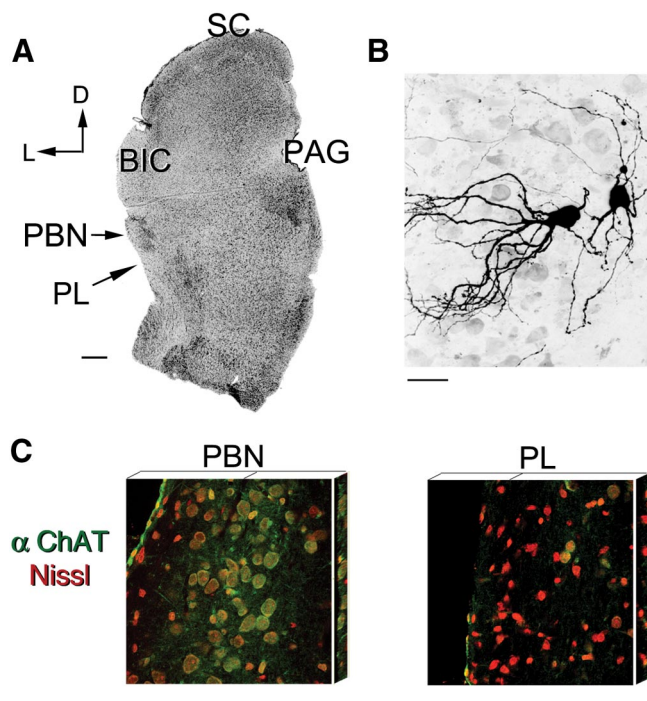
FIG. 1. Parabigeminal nucleus (PBN) neurons in a slice. *A*: image of Nissl-stained, transverse slice of the midbrain containing the parabigeminal nucleus (PBN, arrow). Scale bar = 500 μm. D, dorsal; L, lateral; BIC, brachium of the inferior colliculus; PAG, periacqueductal gray; PL, paralemniscal nucleus; SC, superior colliculus. *B*: biocytin-filled PBN neurons. Two neurons close to each other have distinct morphologies. The dendrites of the neuron on the right have a cylindrical shape, while those of the neuron on the left have a pyramidal shape according to classification of Tokunaga and Otani (1978). The lateral wall of midbrain is to the left. Scale bar = 30 μm. *C*: choline acetyltransferase (ChAT) immunostaining is seen in nearly all somata in the PBN. *Left:* projection of a confocal stack taken through a PBN slice. A cluster of large, green, ChAT-positive somata can be seen overlapping with Nissl stain in red. *Right:* image of the paralemniscal nucleus (PL), which is just ventral to the PBN. Very few of the Nissl-positive cells also colocalize with α-ChAT immunoreactivity. Thin panels on the sides show projections through the confocal stack in the plane of the tick marks. Lateral wall of the midbrain is to the left in both images. Scale bar = 30 μm.

followed by whole cell voltage recordings (Fig. 2*B, bottom right,* mean whole cell firing rate = 3.42 ± 2.55 Hz, $P > 0.45$ compared with cell-attached firing rate, 2-tailed, paired t-test, $n = 15$ neurons). This firing was not due to disruption of the cell membrane in the sealing process or other stresses because tonic firing persisted could be detected for >20 min (Fig. 2*C*). Increasing the temperature of the bath increased spontaneous firing rate (Fig. 2*D*). The firing rate at 32°C was 169 ± 90% of the rate at 24–26°C ($P < 0.01$, $n = 14$ neurons, paired, 1-tailed t-test).

To test whether spontaneous activity results in part from coordinated network activity, paired recordings in PBN neurons were performed. Cell-attached recordings in neighboring neurons failed to demonstrate a correlation in spontaneous firing (Fig. 2*E*, 7/7 pairs). In addition, cross-correlation of the current traces from the paired whole cell recordings did not show evidence of firing coherence, suggesting that PBN neurons did not reliably induce spikes in their neighbors (Fig. 2*E, right*). Only in one neuron did we detect electrical coupling with a neighboring neuron; rhythmic inward currents with rapid rise and fall times, which likely represented action

potentials in a neighboring neuron, were observed in voltage-clamp recordings (data not shown).

Spontaneous activity in PBN neurons does not require fast synaptic input

The spontaneous activity of PBN neurons could be due to synaptic inputs and/or to intrinsic membrane conductances of PBN neurons. Excitatory synaptic inputs are thought to be glutamatergic based on the detection of presynaptically localized vGluT3 protein, but likely arise extrinsically to the nucleus, based on a lack of vGluT3 mRNA in the PBN (Herzog et al. 2004). Intrinsic connections are likely to be cholinergic because most PBN neurons are thought to be cholinergic (Fig. 1*C*) (Mufson et al. 1986) and the presence of α7 subunit containing nicotinic ACh receptors have been reported in the PBN (Tribollet et al. 2004). To determine whether ionotropic input drives the activity of PBN neurons, we tested for spontaneous activity in the presence of synaptic blockers. Cell-attached recordings were made in two conditions: either in the pan-excitatory neurotransmitter receptor blocker, kynurenic acid, or in both the AMPAergic glutamate receptor antagonist, DNQX, and the GABA receptor antagonist, gabazine. Kynurenic acid blocks ionotropic glutamatergic receptors as well as alpha7-subunit containing nicotinic ACh receptors (Collingridge and Lester 1989; Hilmas et al. 2001). Addition of kynurenic acid to the bath blocked spontaneous excitatory postsynaptic currents in PBN neurons (Fig. 3*A*), indicating that these neurons receive fast, excitatory synaptic input. Regular firing persisted in recordings in which the slices were exposed to 1–2 mM kynurenic acid (mean firing rate = 1.9 ± 1.1 Hz, 9/10 neurons). Regular firing also persisted in a combination of DNQX and gabazine in 18 of 18 neurons tested (mean firing rate = 3.6 ± 2.6 Hz). Thus fast synaptic transmission is not required for the generation of rhythmic firing observed in PBN neurons.

To assess a role for cholinergic drive in modulating spontaneous firing, spiking was assessed in seven neurons before and after infusion of a solution containing kynurenic acid (1–2 mM), the α4β2 nicotinic blocker DHβE (100 nM), and the muscarinic ACh receptor antagonist, atropine (1 μM). Spontaneous firing rates were not significantly altered in the presence of these drugs (firing rate with drug was 107 ± 39% of that in the control period, $P > 0.45$; Fig. 3, *B* and *C*). In sum, these experiments indicate that fast synaptic transmission provides a minimal contribution to the spontaneous activity observed in PBN neurons in vitro.

Properties of PBN neurons in response to intracellular current injection

To characterize the firing properties of PBN neurons, neurons were injected with slight hyperpolarizing current to hold the neurons just below action potential threshold and then were given hyper- or depolarizing current injections. In response to a strong hyperpolarizing currents, membrane voltage exhibited an initial hyperpolarization followed by a depolarizing "sag" (Fig. 4*A,* arrow). On termination of the current injection, neurons often fired rebound action potentials. Most neurons (12/14) fired two to four rebound spikes at low frequencies (4.18 ± 1.36 Hz) for several hundreds of milliseconds after the
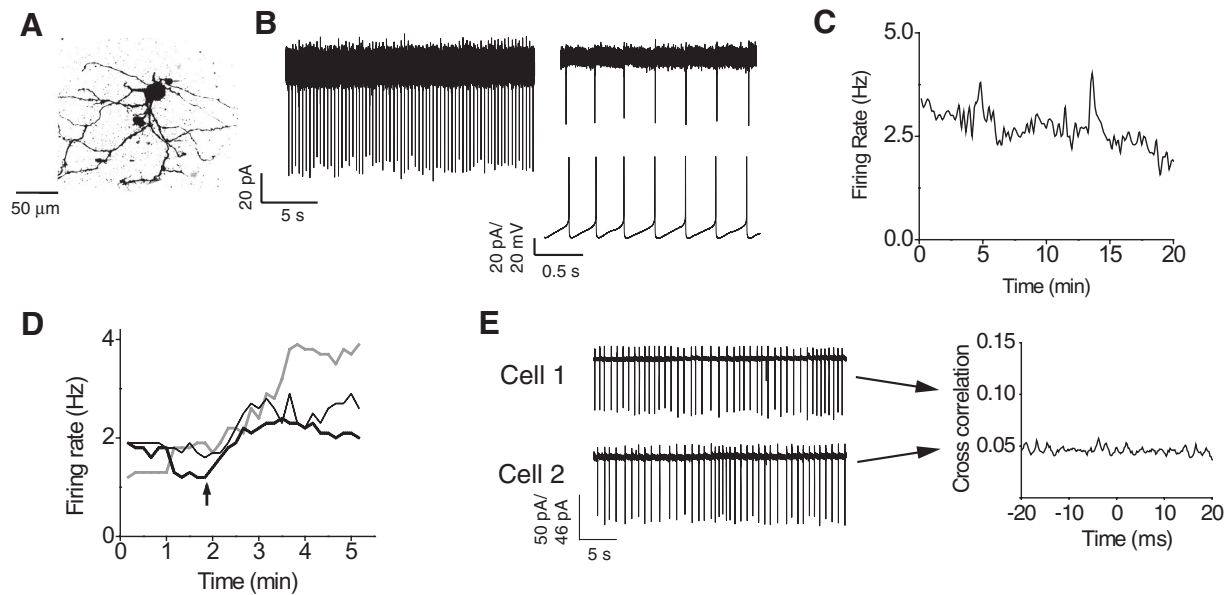
FIG. 2. Spontaneous action potential activity in PBN neurons. *A*: biocytin-filled PBN neuron from which recordings in *B* were made. *B, Left*: 30 s of spontaneous action potentials in a cell-attached patch recording. Firing rate was 3.1 ± 0.2 Hz. *Top right*: 2 s from the *top trace*. Spikes occur rhythmically with a constant rate (2.9 ± 0.3 Hz). *Bottom right*: current-clamp whole cell recording of spontaneous action potentials at a similar rate in the same neuron shown in *A* and *B*. Each spike is followed by a slow voltage ramp until threshold is reached. *C*: example of firing rate over a 20-min period in a current-clamp whole cell recording from a PBN neuron. Firing rate was determined in 10-s bins. Kynurenic acid was added to the bath at minute 2 and remained present for the duration of the recording. *D*: firing rate is sensitive to bath temperature. Three different example neurons are shown. Firing rate is steady in each cell at 26°C from 0 to 2 min. Firing rate increases after artificial cerebrospinal fluid (ACSF) was warmed to 32°C ($\rightarrow$). Across all neurons tested, the firing rate at 32°C was $169 \pm 90\%$ of the rate at 24–26°C ($P < 0.01$, $n = 14$ neurons, paired, 1-tailed *t*-test). *E*: paired cell-attached patch-clamp recordings. *Left:* representative recordings of 2 neighboring neurons in the PBN that do not fire in phase or at the same frequency. *Right:* cross-correlation of *cell 1* activity with cell 2 activity. The firing of these neighboring neurons was not correlated.

termination of the hyperpolarizing step, and a minority (2/14) fired high-frequency bursts of two to three spikes (>60 Hz) at much shorter (<50 ms) latencies. Preceding the low-frequency rebound spikes, a slow, depolarizing voltage ramp was observed that delayed the onset of spiking; this behavior is characteristic of I_A (Fig. 4*A,* open arrowhead) (Jan and Jan 1989; Rogawski 1985).

In response to a depolarizing current injection, PBN neurons fired action potentials tonically (Fig. 4*A;* mean frequency in response to 100-pA current injection: 27.2 ± 10.7 Hz, range: 12.5–47.2 Hz, $n = 19$ neurons). During a 1-s current injection, the firing rate accommodated slightly: the firing rate at the end of current injection was $82 \pm 16\%$ of the rate at the beginning of the current injection ($P < 0.03$, $n = 19$ neurons).

Intrinsic currents in PBN neurons: I_H

Because fast synaptic transmission is not required for the spontaneous, regular firing of PBN neurons in vitro, intrinsic conductances are most likely responsible. Several currents that are implicated in rhythmic action potential generation can be elicited by membrane hyperpolarization or after the return from a hyperpolarizing step. Using whole cell patch-clamp recordings, we characterized several currents activated in response to hyperpolarizing pulses. During a 1-s, hyperpolarizing pulse, a pronounced inward current was observed (Fig. 4*B*, left arrow). It appeared to be an H current (I_H) because it was inward, hyperpolarization-activated, and did not inactivate. I_H persisted throughout the hyperpolarizing pulse, and a several-second
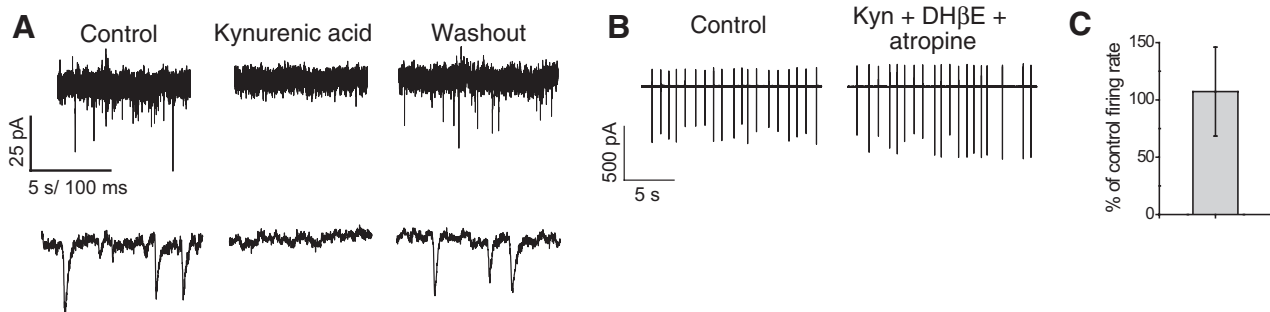

FIG. 3. Synaptic inputs are not required for spontaneous firing of PBN neurons. *A*: kynurenic acid is effective in blocking ionotropic synaptic activity in PBN neurons during whole cell voltage-clamp recordings ($n = 3$ neurons). *Top*: responses over 10 s; *bottom*: selected events on an expanded time scale over 200 ms. Control: spontaneous inward currents can be detected in control ACSF at a holding potential of -65 mV. Kynurenic acid: inward currents disappear in the presence of 2 mM kynurenic acid. Washout: inward currents reappear after washout of kynurenic acid. *B*: addition of the pan-ionotropic excitatory neurotransmitter receptor blocker kynurenic acid (1–2 mM), dihydro-beta-erythroidine (DHβE, 100 nM), and atropine (1 μM) did not prevent spontaneous, rhythmic action potential generation detected with a cell-attached patch-clamp recordings. *Right*: taken 4 min after infusion of drugs. *C*: quantification of firing rate after infusion of kynurenic acid, DHβE, and atropine. Firing rate in drug cocktail was $107 \pm 39\%$ of that in the control period, $P > 0.4$, $n = 7$ neurons.
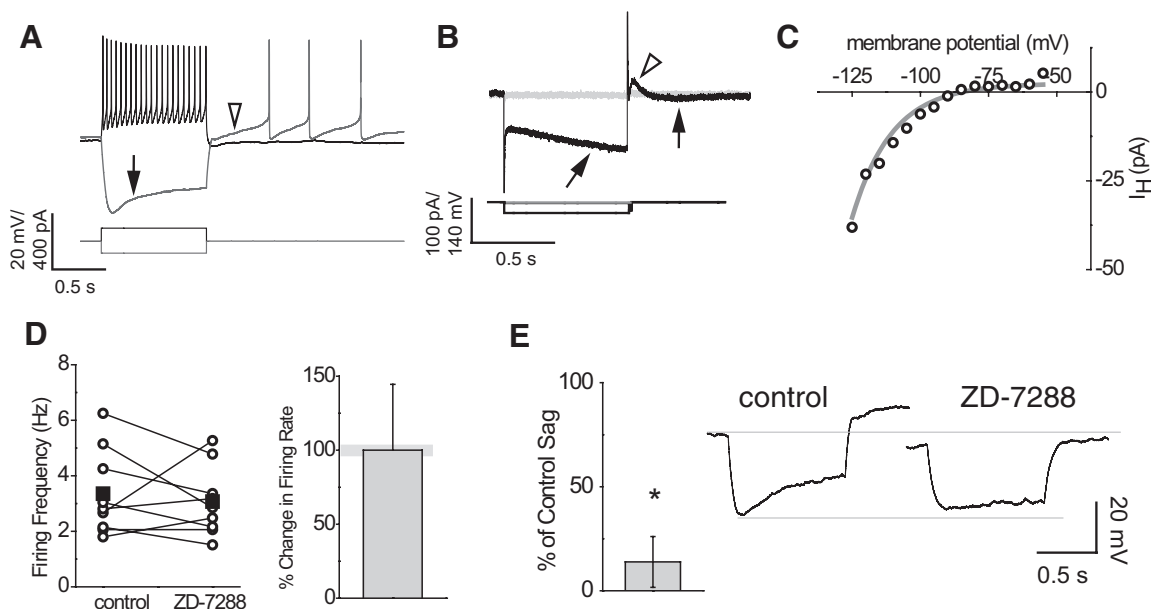
FIG. 4. Voltage-activated intrinsic currents in PBN neurons. *A*: response of a PBN neuron to current injections in a whole cell voltage recording. Spontaneous firing was suppressed by continuously injecting a small amount of hyperpolarizing current. With an additional injection of depolarizing current for 1 s, a steady train of action potentials was produced with little accommodation (black trace). In response to a hyperpolarizing current injection (gray trace), the membrane responded first with an immediate hyperpolarization followed by a depolarizing sag (arrow). On release from the current injection, the membrane returned back to rest, and then slowly depolarized (open arrowhead) to the point of firing a few action potentials (Fig. 2*B*). *B*: several intrinsic currents are detected in voltage-clamp recordings from PBN neurons in response to a hyperpolarizing voltage step to -125 mV and on return to -65 mV. A slowly activating and slowly deactivating inward I_H current is observed (arrows) during and after the voltage step. I_H observed at a holding potential of -125 mV had a slow onset (time constant of activation: 620 ± 220 ms, $n = 10$ neurons). A faster I_A current is deinactivated during the hyperpolarizing voltage step and is transiently activated on stepping the membrane back to -65 mV (open arrowhead). *C*: deinactivation range of I_H in PBN neurons. Membrane potential during the hyperpolarizing pulse is plotted on the abscissa; the difference in current between the first 50 ms and last 50 ms of the hyperpolarizing pulse is plotted on the ordinate. Dark circles represent the I_H curve for one example cell. Gray curve represents a polynomial fit of I_H curves from 13 neurons; significant current was not detected unless the membrane potential was below -85 mV. *D*: effect of 25 μM ZD-7288 on spontaneous firing rate. *Left:* open circles connected by line indicate firing rates before and after ZD-7288 application; filled squares indicate the average firing rate in each condition. These recordings were performed in the presence of DNQX and gabazine to block synaptic input. Control firing rate (3.3 ± 1.5 Hz) is not significantly different from firing rate after ZD-7288 application (3.1 ± 1.3 Hz; $P > 0.5$, paired, 2-tailed t-test, $n = 9$ neurons) *Right:* average change in firing rate after ZD-7288 application: rate in ZD-7288 is $100 \pm 44\%$ of control. *E, left:* quantification of change in membrane potential sag after application of ZD-7288. Sag in ZD-7288 is reduced to $13 \pm 12\%$ of that observed in control ($P < 0.001$, paired, 1-tailed t-test, $n = 8$ neurons). *Right:* representative example traces depict changes in I_H membrane sag after application of 25 μM ZD-7288.

long tail current was observed after the cell was returned to a holding potential near rest (Fig. 4*B*, right arrow). This current is the counterpart to the depolarizing membrane sag observed in current-clamp recordings (Fig. 4*A*, arrow). The activation range of I_H was quite hyperpolarized as significant current was activated only with hyperpolarizations beyond -85 mV (Fig. 4*C*). A brief, outward current was also detected on returning the cell back to -65 mV (Fig. 4*B*, open arrowhead); this current will be discussed in the next section.

To test whether I_H contributed to the spontaneous activity observed in PBN neurons, we monitored the spontaneous firing rate during the application of the I_H blocker, ZD-7288, to the bath. These recordings were performed in the presence of DNQX and gabazine to block synaptic transmission. Application of 25 μM ZD-7288 neither prevented the spontaneous activity of PBN neurons nor did it significantly modulate the firing rate (Fig. 4*D*). The mean firing rate was 3.35 ± 1.53 Hz in the control condition and was 3.07 ± 1.25 Hz after application of ZD-7288 ($P > 0.5$, paired, 2-tailed t-test, $n = 9$ neurons).

To be sure that ZD-7288 was inhibiting I_H, we tested whether hyperpolarization-induced membrane potential sag, indicative of I_H, was affected by the application of 25 μM ZD-7288 (Fig. 4*E*). We tested whether an I_H-related sag was reduced by ZD-7288 in eight neurons; in six of these neurons,

we monitored spontaneous firing. Membrane sag after ZD-7288 application was reduced to $13.9 \pm 12.2\%$ of that in the control condition ($P < 0.001$, paired, 1 tailed t-test, $n = 8$ neurons). In sum, although ZD-7288 blocked I_H, it did not alter the spontaneous firing rate in PBN neurons.

Intrinsic currents in PBN neurons: I_A

The slow rise of the voltage ramp observed in current-clamp recordings between spontaneously occurring action potentials (Fig. 5*A*, open arrowhead) and on a termination of hyperpolarizing current pulse (Fig. 4*A*, open arrowhead) is indicative of A-type K^+ current (I_A). As mentioned previously, a transient outward current was observed in voltage-clamp recordings after a long hyperpolarizing pulse (Fig. 4*B*, open arrowhead). With a short (100 ms), hyperpolarizing pulse that did not activate I_H significantly, I_A was obtained in isolation (Fig. 5*B*, open arrowhead). I_A peaked 25 ± 3 ms following the voltage activation step ($n = 7$) and lasted roughly 100–200 ms. This current was consistent with an A-type K^+ current (Rogawski 1985); it was brief, it rapidly recovered from inactivation by brief hyperpolarizing pulses and was activated by modest depolarizations to membrane potentials near -65 mV. Due to presence of active Na^+ conductances in the neurons, it was not possible to adequately clamp voltage at more depolarized
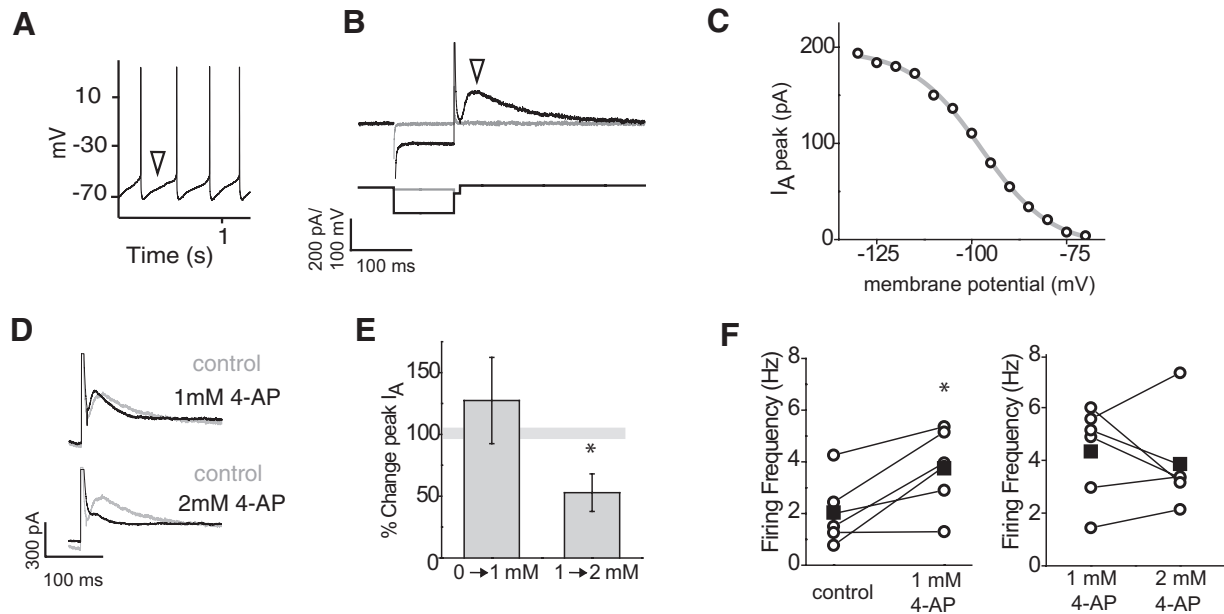
FIG. 5. I_A currents in PBN neurons. *A*: current-clamp recording of spontaneous activity in a PBN neuron. The trough of the afterhyperpolarization is at about −70 mV. Open arrowhead points to slow a voltage ramp between spikes. *B*: isolation of I_A in PBN neurons. I_A (open arrowhead) is isolated by a brief, conditioning (100 ms) hyperpolarizing pulse, followed by a step back to −55 mV. *C*: steady-state inactivation curve for I_A in PBN neurons. The membrane potential during the conditioning hyperpolarizing pulse is plotted on the abscissa. The average peak I_A value is plotted on the ordinate. Dark circles represent peak I_A for 1 example cell and the gray curve is a Boltzmann curve fit to that cell. For this cell, the Boltzmann parameters were: max current = 196 pA; V_m at half max = −97.5 mV; curve width = 9.2 mV. For 19 neurons, mean Boltmann parameters were: max current = 215 ± 81 pA; V_m at half max = −96.4 ± 3.6 mV; curve width = 10.4 ± 1.7 mV. *D*: representative traces depicting I_A in control and after application of 1 or 2 mM 4-aminopyridine (4-AP). *E*: quantification of I_A for 6 neurons sequentially treated with 1 mM 4-AP, then 2 mM 4-AP. I_A peak amplitude after application of 1 mM 4-AP was 127 ± 35% of control (2-tailed paired t-test, $P > 0.1$). I_A peak amplitude after application of 2 mM 4-AP was 53 ± 15% of I_A in 1 mM 4-AP (asterisk denotes significance by 2-tailed paired t-test, $P < 0.01$, $n = 6$). *F*: firing frequency for neurons treated with 1 and 2 mM 4-AP. Open circles connected by lines indicate firing rates before and after 4-AP application; filled squares indicate the average firing rate in each condition. These recordings were performed in the presence of 6,7-dinitroquinoxaline-2,3-dione (DNQX) and gabazine to block synaptic input. *Left*: firing rate increased from 2.0 ± 1.5 Hz in control to 3.7 ± 2.3 Hz in 1 mM 4-AP ($n = 6$ neurons, asterisk denotes significance by paired t-test, $P = < 0.02$). *Right*: firing rates were not different in neurons treated sequentially with 1 mM (4.3 ± 1.8 Hz) and 2 mM 4-AP (3.9 ± 1.8 Hz, $n = 6$ neurons, 2-tailed paired t-test, $P > 0.5$).

membrane potentials to obtain the complete activation range for I_A. A steady-state inactivation voltage protocol, consisting of 100-ms conditioning steps (voltage range of −100 to −60 mV) followed by a test step to −60 or −55 mV revealed that I_A was half inactivated at −97 mV and that detectable current could be activated after modest membrane hyperpolarization of −70 mV (Fig. 5*C*), which is near the trough voltage obtained during spontaneous firing (Fig. 5*A*). Thus I_A is another intrinsic current that could regulate spontaneous firing of PBN neurons.

To assess whether I_A regulated the firing rate of PBN neurons, we applied 4-AP to the bath. These recordings were performed in the presence of DNQX and gabazine to block synaptic input. As relatively high concentrations of 4-AP are sometimes required to block I_A (Rogawski 1985), we first determined a concentration of 4-AP necessary to reduce I_A in PBN neurons. Application of 1 mM 4-AP did not significantly reduce I_A (Fig. 5, *D* and *E*). With a deinactivation pulse to −130 mV and a test pulse to −65 or −60 mV, peak I_A in control was 139.8 ± 62.8 pA and in 1 mM 4-AP was 162.7 ± 50.0 pA ($P > 0.15$, paired, 2-tailed t-test, $n = 6$). However, on increasing 4-AP to 2 mM, I_A was significantly reduced by 53 ± 15% to 80 ± 11 pA ($P < 0.01$, paired, 2-tailed t-test, Fig. 5, *D* and *E*). Thus 2 mM 4-AP was a concentration required to effectively reduce I_A in PBN neurons.

We then tested if 4-AP blockade of I_A results in a significant change in firing rate. Because 4-AP can block many types of K^+ channels that affect excitability (Judge and Bever 2006), we first

assessed the effect of 1 mM 4-AP on PBN firing rate, then incremented the concentration of 4-AP to 2 mM. In this way, we hoped to control for as many of the non-I_A-dependent effects of 4-AP by initially using a concentration that does not significantly affect I_A, then increased the concentration of 4-AP to an I_A-effective concentration. Addition of 1 mM 4-AP caused a significant increase in the firing rate of PBN neurons (Fig. 5*F, left*), from 2.0 ± 1.5 Hz in control conditions to 3.7 ± 2.3 Hz in 1 mM 4-AP ($n = 6$ neurons, $P < 0.02$, 2-tailed paired t-test), but further increasing the concentration from 1 to 2 mM caused highly variable effects on PBN neurons, including depolarization block in four of six cases. The net effect on firing rate in 2 mM 4-AP was not significant different from 1 mM 4-AP (3.9 ± 1.8 Hz, $n = 6$ neurons, 2-tailed paired t-test, $P > 0.5$). However, as these high concentrations of 4-AP substantially altered neuronal function independent of I_A blockade, we were unable to demonstrate conclusively a role for I_A in regulating the spontaneous firing.

DISCUSSION

Here we report that PBN neurons fire spontaneous, regular action potentials in vitro. This spontaneous activity was generated independently of fast synaptic input. Two intrinsic currents were observed in PBN neurons that are known to play a role in the regulation of spontaneous activity in various neurons.

PBN neurons have been shown to be cholinergic from ChAT immunoreactivity studies (Beninato and Spencer 1986; Mufson

et al. 1986). Consistent with previous studies, we find that the PBN contains a high proportion of ChAT immunoreactive neurons. Moreover, the morphology of biocytin filled neurons reported here (Figs. 1 and 2) are consistent with those reported in Golgi studies of PBN (Tokunaga and Otani 1978).

The underlying mechanisms of spontaneous firing in the PBN may be similar to those demonstrated in other nuclei that exhibit spontaneous neuronal firing, such as in cerebellum (Raman and Bean 1999), hypothalamus (Jackson et al. 2004), striatum (Wilson 2005), and many other nuclei (Llinas 1988), where dynamic interactions between Na^+ and K^+ conductances foster ongoing activity. We found that PBN neurons have I_H and I_A. These currents have been shown to contribute to and/or modulate spontaneous firing in various neuronal types, so we tested their role in spontaneous firing in PBN neurons. The A-current observed in these studies (Fig. 5) is likely to be deinactivated during the spike afterhyperpolarization of the neuron. The slow depolarizing voltage ramp observed after each action potential (Fig. 5A) and after a prolonged hyperpolarization (Fig. 4D) are characteristic of I_A (Connor and Stevens 1971; Rogawski 1985). I_A has been shown to allow slow, repetitive firing of neurons (Bourdeau et al. 2007; Nisenbaum et al. 1994). Similarly, PBN neurons are able to fire in a slow, tonic fashion. The I_A observed here is activated by membrane depolarizations to approximately −65 mV and is deinactivated by modest hyperpolarizations to −70 mV (Fig. 5C). Thus I_A is active in the range of membrane voltages observed during the spike afterhyperpolarization and may participate in the generation and pacing of the spontaneous firing in PBN neurons.

However, our tests to demonstrate the role of I_A in regulating PBN neuron firing with 4-AP were inconclusive. 4-AP is known to block various K^+ channels, including those with A-type properties, in the submillimolar range (Judge and Bever 2006; Rogawski 1985; Russell et al. 1994). Our observation that 1 mM 4-AP increased firing rate is consistent with the general increase in excitability that accompanies K^+ blockade. However, 2 mM 4-AP was required to effectively reduce I_A in PBN neurons. This high concentration of 4-AP severely disrupted action potential generation in a manner consistent with a persistent inactivation of Na^+ channels. Moreover, the action of 4-AP may be to enhance, not inhibit, I_A in response to slow voltage ramps, similar to those observed during the PBN interspike interval (A. C. Jackson, personal communication). To more completely assess the contribution of I_A to spontaneous firing in these neurons, either new pharmacological agents or genetic manipulation of specific A-type K^+ channels will be required. The observation that A-type current in PBN neurons is blocked by millimolar concentrations of 4-AP suggests that this current is carried by Kv 4.x subunit-containing channels, not Kv 1.x-containing channels (Coetzee et al. 1999).

I_H has been shown to contribute to pacemaking firing pattern in various groups of neurons (Chan et al. 2004; Luthi and McCormick 1998) and has been observed in other cholinergic nuclei (Gorelova and Reiner 1996; Griffith and Matthews 1986). However, the voltage range of I_H activation observed here suggests that it does not contribute significantly to the spontaneous firing of PBN neurons in vitro; the activation range of the I_H is significantly hyperpolarized (less than −85 mV) relative to the trough of the spike afterhyperpolarization, which was about −70 mV (Fig. 4A). Consistent with this

interpretation, application of 25 μM ZD-7288, which effectively blocked I_H, did not alter firing rate. These results are similar to those obtained in a subset of hippocampal interneurons that express an I_H that does not appear to contribute to the rhythmic firing observed those neurons (Bourdeau et al. 2007). Although we have not demonstrated it here, I_H could play a role in repolarizing the neuron after a strong wave of GABAergic inhibition and could even induce rebound spikes.

The observation that PBN neurons fire spontaneously in vitro is consistent with prior reports of spontaneous activity in vivo. However, the rate of spontaneous firing in the rat PBN in vitro was significantly lower than that observed in cats in vivo; cat PBN neurons fired spontaneously at ∼15 Hz, with a range from 0 to >50 Hz (Cui and Malpeli 2003; Sherk 1979). This difference may be partially due to species differences but is most likely due to the effects of slicing; intrinsic properties of the neurons may be altered due to bath conditions and synaptic drive not maintained in the slice preparation that could contribute to an increased firing rate. However, our data suggest that even in the deafferented slice, in which extrinsic neuromodulatory influences are negligible, intrinsic mechanisms exist that promote continuous firing of PBN neurons.

The function of spontaneous activity in the PBN is not known, although it has been postulated that it may help PBN neurons respond very rapidly to sensory inputs (Sherk 1979). Moreover, the presence of spontaneous activity enables neurons to represent both increases and decreases of synaptic drive to their target. Evidence of this type of push-pull regulation of firing in the PBN has been observed in vivo in response to moving visual stimuli (Cui and Malpeli 2003). Targets moving in the appropriate hemifield elicit a high firing rate in the PBN, but targets moving in the opposite hemifield completely silence the neuron. Thus levels of ACh in SC can be dynamically regulated by controlling the activity of the PBN.

Spontaneous firing occurs frequently in neuromodulatory regions, such as the suprachiasmatic nucleus (Jackson et al. 2004; Pennartz et al. 1997) and in dopaminergic centers (Koyama et al. 2005; Puopolo et al. 2007). It is likely that the PBN is acting as a modulator of SC activity. ACh infusion depolarizes some types of principal neurons as well as affects the release of GABA onto various types of SC neurons (Endo et al. 2005; Lee et al. 2001; Li et al. 2004). The finding that the PBN is spontaneously active implies that the PBN delivers a continuous, low level of ACh to the SC. However, the specific effect of PBN activity on SC circuits has not yet been established. Neurons in other cholinergic nuclei have been reported to exhibit spontaneous firing, suggesting that this tonic release of ACh may be a general mechanism for cholinergic modulation (Arrigoni et al. 2006; Wilson 2005).

The PBN is the mammalian analogue of the nucleus isthmi, a complex of nuclei found in nonmammalian vertebrates. In particular, PBN appears to be closely related to the nucleus isthmi pars parvocellularis (Ipc) (Wang et al. 2006). Neurons in Ipc fire high-frequency bursts of action potentials in response to visual or auditory input; they also fire spontaneously in the absence of sensory input (Maczko et al. 2006; Marin et al. 2005). Moreover, Ipc activity can facilitate calcium entry into presynaptic terminals in the frog tectum, a structure analogous to mammalian SC (Dudkin and Gruberg 2003). These observations suggest that the function of PBN and Ipc may be similar. Future work will determine the functional similarity of these structures.

REFERENCES

Aizawa H, Kobayashi Y, Yamamoto M, Isa T. Injection of nicotine into the superior colliculus facilitates occurrence of express saccades in monkeys. *J Neurophysiol* 82: 1642–1646, 1999.

Arrigoni E, Chamberlin NL, Saper CB, McCarley RW. Adenosine inhibits basal forebrain cholinergic and noncholinergic neurons in vitro. *Neuroscience* 140: 403–413, 2006.

Beninato M, Spencer RF. A cholinergic projection to the rat superior colliculus demonstrated by retrograde transport of horseradish peroxidase and choline acetyltransferase immunohistochemistry. *J Comp Neurol* 253: 525–538, 1986.

Bourdeau ML, Morin F, Laurent CE, Azzi M, Lacaille, J.-C. Kv4.3-mediated A-type K^+ currents underlie rhythmic activity in hippocampal interneurons. *J Neurosci* 27: 1942–1953, 2007.

Chan CS, Shigemoto R, Mercer JN, Surmeier DJ. HCN2 and HCN1 channels govern the regularity of autonomous pacemaking and synaptic resetting in globus pallidus neurons. *J Neurosci* 24: 9921–9932, 2004.

Coetzee WA, Amarillo Y, Chiu J, Chow A, Lau D, McCormack T, Moreno H, Nadal MS, Ozaita A, Pountney D, Saganich M, Vega-Saenz de Miera E, Rudy B. Molecular diversity of K^+ channels. *Ann NY Acad Sci* 868: 233–285, 1999.

Collingridge GL, Lester RA. Excitatory amino acid receptors in the vertebrate central nervous system. *Pharmacol Rev* 41: 143–210, 1989.

Connor JA, Stevens CF. Prediction of repetitive firing behaviour from voltage clamp data on an isolated neuron soma. *J Physiol* 213: 31–53, 1971.

Cui H, Malpeli JG. Activity in the parabigeminal nucleus during eye movements directed at moving and stationary targets. *J Neurophysiol* 89: 3128–3142, 2003.

Drager UC, Hubel DH. Responses to visual stimulation and relationship between visual, auditory, and somatosensory inputs in mouse superior colliculus. *J Neurophysiol* 38: 690–713, 1975.

Dudkin EA, Gruberg ER. Nucleus isthmi enhances calcium influx into optic nerve fiber terminals in *Rana pipiens. Brain Res* 969: 44–52, 2003.

Endo T, Yanagawa Y, Obata K, Isa T. Nicotinic acetylcholine receptor subtypes involved in facilitation of GABAergic inhibition in mouse superficial superior colliculus. *J Neurophysiol* 94: 3893–3902, 2005.

Gorelova N, Reiner PB. Role of the afterhyperpolarization in control of discharge properties of septal cholinergic neurons in vitro. *J Neurophysiol* 75: 695–706, 1996.

Graybiel AM. A satellite system of the superior colliculus: the parabigeminal nucleus and its projections to the superficial collicular layers. *Brain Res* 145: 365–374, 1978.

Griffith WH, Matthews RT. Electrophysiology of AChE-positive neurons in basal forebrain slices. *Neurosci Lett* 71: 169–174, 1986.

Harting JK, Hashikawa T, Van Lieshout D. Laminar distribution of tectal, parabigeminal and pretectal inputs to the primate dorsal lateral geniculate nucleus: connectional studies in *Galago crassicaudatus. Brain Res* 366: 358–363, 1986.

Hashikawa T, Van Lieshout D, Harting JK. Projections from the parabigeminal nucleus to the dorsal lateral geniculate nucleus in the tree shrew *Tupaia glis. J Comp Neurol* 246: 382–394, 1986.

Hasselmo ME, McGaughy J. High acetylcholine levels set circuit dynamics for attention and encoding and low acetylcholine levels set dynamics for consolidation. *Prog Brain Res* 145: 207–231, 2004.

Herzog E, Gilchrist J, Gras C, Muzerelle A, Ravassard P, Giros B, Gaspar P, El Mestikawy S. Localization of VGLUT3, the vesicular glutamate transporter type 3, in the rat brain. *Neuroscience* 123: 983–1002, 2004.

Hilmas C, Pereira EF, Alkondon M, Rassoulpour A, Schwarcz R, Albuquerque EX. The brain metabolite kynurenic acid inhibits alpha7 nicotinic receptor activity and increases non-alpha7 nicotinic receptor expression: physiopathological implications. *J Neurosci* 21: 7463–7473, 2001.

Isa T. Intrinsic processing in the mammalian superior colliculus. *Curr Opin Neurobiol* 12: 668–677, 2002.

Jackson AC, Yao GL, Bean BP. Mechanism of spontaneous firing in dorsomedial suprachiasmatic nucleus neurons. *J Neurosci* 24: 7985–7998, 2004.

Jan LY, Jan YN. Voltage-sensitive ion channels. *Cell* 56: 13–25, 1989.

Judge SI, Bever CT Jr. Potassium channel blockers in multiple sclerosis: neuronal Kv channels and effects of symptomatic treatment. *Pharmacol Ther* 111: 224–259, 2006.

Koyama S, Kanemitsu Y, Weight FF. Spontaneous activity and properties of two types of principal neurons from the ventral tegmental area of rat. *J Neurophysiol* 93: 3282–3293, 2005.

Lee P, Hall WC. An in vitro study of horizontal connections in the intermediate layer of the superior colliculus. *J Neurosci* 26: 4763–4768, 2006.

Lee PH, Schmidt M, Hall WC. Excitatory and inhibitory circuitry in the superficial gray layer of the superior colliculus. *J Neurosci* 21: 8145–8153, 2001.

Li F, Endo T, Isa T. Presynaptic muscarinic acetylcholine receptors suppress GABAergic synaptic transmission in the intermediate grey layer of mouse superior colliculus. *Eur J Neurosci* 20: 2079–2088, 2004.

Llinas RR. The intrinsic electrophysiological properties of mammalian neurons: insights into central nervous system function. *Science* 242: 1654–1664, 1988.

Luthi A, McCormick DA. H-current: properties of a neuronal and network pacemaker. *Neuron* 21: 9–12, 1998.

Maczko KA, Knudsen PF, Knudsen EI. Auditory and visual space maps in the cholinergic nucleus isthmi pars parvocellularis of the barn owl. *J Neurosci* 26: 12799–12806, 2006.

Marin G, Mpodozis J, Sentis E, Ossandon T, Letelier JC. Oscillatory bursts in the optic tectum of birds represent re-entrant signals from the nucleus isthmi pars parvocellularis. *J Neurosci* 25: 7081–7089, 2005.

Mufson EJ, Martin TL, Mash DC, Wainer BH, Mesulam MM. Cholinergic projections from the parabigeminal nucleus (Ch8) to the superior colliculus in the mouse: a combined analysis of horseradish peroxidase transport and choline acetyltransferase immunohistochemistry. *Brain Res* 370: 144–148, 1986.

Muller JR, Philiastides MG, Newsome WT. Microstimulation of the superior colliculus focuses attention without moving the eyes. *Proc Natl Acad Sci USA* 102: 524–529, 2005.

Nisenbaum ES, Xu ZC, Wilson CJ. Contribution of a slowly inactivating potassium current to the transition to firing of neostriatal spiny projection neurons. *J Neurophysiol* 71: 1174–1189, 1994.

Pennartz CM, Bierlaagh MA, Geurtsen AM. Cellular mechanisms underlying spontaneous firing in rat suprachiasmatic nucleus: involvement of a slowly inactivating component of sodium current. *J Neurophysiol* 78: 1811–1825, 1997.

Puopolo M, Raviola E, Bean BP. Roles of subthreshold calcium current and sodium current in spontaneous firing of mouse midbrain dopamine neurons. *J Neurosci* 27: 645–656, 2007.

Raman IM, Bean BP. Ionic currents underlying spontaneous action potentials in isolated cerebellar Purkinje neurons. *J Neurosci* 19: 1663–1674, 1999.

Rogawski MA. The A-current: how ubiquitous a feature of excitable cells is it? *Trends Neurosci* 8: 214–219, 1985.

Russell SN, Publicover NG, Hart PJ, Carl A, Hume JR, Sanders KM, Horowitz B. Block by 4-aminopyridine of a Kv1.2 delayed rectifier K^+ current expressed in *Xenopus* oocytes. *J Physiol* 481: 571–584, 1994.

Sherk H. A comparison of visual-response properties in cat's parabigeminal nucleus and superior colliculus. *J Neurophysiol* 42: 1640–1655, 1979.

Tokunaga A, Otani K. Neuronal organization of the corpus parabigeminum in the rat. *Exp Neurol* 58: 361–375, 1978.

Tribollet E, Bertrand D, Marguerat A, Raggenbass M. Comparative distribution of nicotinic receptor subtypes during development, adulthood and aging: an autoradiographic study in the rat brain. *Neuroscience* 124: 405–420, 2004.

Usunoff KG, Itzev DE, Rolfs A, Schmitt O, Wree A. Brain stem afferent connections of the amygdala in the rat with special references to a projection from the parabigeminal nucleus: a fluorescent retrograde tracing study. *Anat Embryol* 211: 475–496, 2006.

Wang Y, Luksch H, Brecha NC, Karten HJ. Columnar projections from the cholinergic nucleus isthmi to the optic tectum in chicks (*Gallus gallus*): a possible substrate for synchronizing tectal channels. *J Comp Neurol* 494: 7–35, 2006.

Wilson CJ. The mechanism of intrinsic amplification of hyperpolarizations and spontaneous bursting in striatal cholinergic interneurons. *Neuron* 45: 575–585, 2005.